Cathepsin cysteine proteases are effectors of invasive growth and angiogenesis during multistage tumorigenesis

Johanna A. Joyce,[1,2] Amos Baruch,[1,4] Kareem Chehade,[1,4] Nicole Meyer-Morse,[1,2] Enrico Giraudo,[1,2] Fong-Ying Tsai,[3] Doron C. Greenbaum,[1] Jeffrey H. Hager,[1,2] Matthew Bogyo,[1,5,*] and Douglas Hanahan[1,2,*]

[1]Department of Biochemistry and Biophysics
[2]Diabetes and Comprehensive Cancer Centers
University of California at San Francisco, 513 Parnassus Avenue, San Francisco, California 94143
[3]Millenium Pharmaceuticals Inc., 75 Sidney Street, Cambridge, Massachusetts 02139
[4]Present address: Celera Genomics, 180 Kimball Way, South San Francisco, California 94080
[5]Present address: Department of Pathology, Stanford Medical School, 300 Pasteur Drive, Stanford, California 94305
*Correspondence: mbogyo@stanford.edu (M.B.); dh@biochem.ucsf.edu (D.H.)

Summary

Tumors develop through successive stages characterized by changes in gene expression and protein function. Gene expression profiling of pancreatic islet tumors in a mouse model of cancer revealed upregulation of cathepsin cysteine proteases. Cathepsin activity was assessed using chemical probes allowing biochemical and in vivo imaging, revealing increased activity associated with the angiogenic vasculature and invasive fronts of carcinomas, and differential expression in immune, endothelial, and cancer cells. A broad-spectrum cysteine cathepsin inhibitor was used to pharmacologically knock out cathepsin function at different stages of tumorigenesis, impairing angiogenic switching in progenitor lesions, as well as tumor growth, vascularity, and invasiveness. Cysteine cathepsins are also upregulated during HPV16-induced cervical carcinogenesis, further encouraging consideration of this protease family as a therapeutic target in human cancers.

Introduction

Cancer is a complex set of proliferative diseases that are thought to arise in most cases via multistep pathways involving an accumulation of genetic and epigenetic changes, including inactivation of tumor suppressor genes and activation of oncogenes (Hanahan and Weinberg, 2000; Kinzler and Vogelstein, 1996). The development of tumors can be separated into a series of distinct clinical, histological, and temporal stages. Mouse models of multistage carcinogenesis allow the study of the molecular basis of this process, and the identification and characterization of molecular effectors of cancer in many organs (Wu and Pandolfi, 2001).

RIP1-Tag2 transgenic mice develop multiple pancreatic islet tumors by 12–14 weeks of age, as a consequence of expressing the SV40 T antigen (Tag) oncogenes in insulin-producing β cells (Hanahan, 1985). Tumor development in these mice proceeds through a series of discrete stages, in which approximately 50% of the ~400 islets in the pancreas become hyperproliferative, of which a subset (~25%) subsequently acquire the ability to switch on angiogenesis (Folkman et al., 1989). A subset of these angiogenic islets (15%–20%) develop into tumors; both benign, encapsulated lesions and invasive carcinomas (Lopez and Hanahan, 2002). This multistage pathway suggests the sequential involvement of multiple rate-limiting genetic and epigenetic events in the progression from normal cells to tumors.

To define novel molecular pathways to cancer, we sought to profile changes in gene expression in each of the lesional stages of sequential tumor development in RIP1-Tag2 mice. We present evidence that a subset of papain family Clan CA cysteine proteases known as cathepsins make an important contribution to the development of islet tumors. The traditional term "cathepsin" includes serine, cysteine, and aspartyl type proteases. The work presented here focuses on the cysteine cathepsin family, which comprises 11 human members to date (cathepsins B, C, H, F, K, L, O, S, V, W, and X/Z) (Turk et al., 2002), and will be collectively abbreviated hereafter simply as cathepsins. These cathepsins are primarily intracellular proteases that function in terminal protein degradation in lysosomes

SIGNIFICANCE

The use of chemical tools to evaluate biological systems is affording powerful means to investigate cellular processes, signaling networks, and molecular mechanisms. In this study, activity-based probes and a class-specific small molecule inhibitor were used to investigate the functional importance of the cathepsin cysteine proteases in cancer. Imaging of cysteine cathepsin activity in vivo revealed pronounced upregulation in precursor and neoplastic lesions of the endocrine pancreas and uterine cervix in two mouse models of multistage cancer, with activity localized to the angiogenic vasculature and invasive fronts of tumors. Correspondingly, pharmacological inhibition of cysteine cathepsin activity impaired angiogenic switching, tumor growth, and invasion in the pancreatic model. The results collectively motivate therapeutic investigation of cysteine cathepsin inhibitors in human cancers.

(Turk et al., 2001) and protein processing in other intracellular organelles (e.g., hormone secretory granules [Yasothornsrikul et al., 2003]). However, cathepsins have specific roles in physiological processes, including bone remodeling, epidermal homeostasis, and antigen presentation (reviewed in Turk et al., 2002). Enzymes of this group can be found at the cell surface, both in T cells (Balaji et al., 2002) and in certain tumors (reviewed in Roshy et al., 2003), and in some cases are secreted (Brix et al., 2001; Koblinski et al., 2002; Mort et al., 1985; Recklies et al., 1985). Surveys of human tumors have suggested an association of certain cathepsins with malignancy (Lah and Kos, 1998; Rao, 2003; Yan et al., 1998), but this class of proteases has not been a prominent target for anticancer therapies, in contrast to the matrix metalloproteases. We show here using small molecule inhibitors and activity based probes that cathepsin activity is increased during tumorigenesis and that inhibition of cathepsin function impairs tumor development.

Results

Cathepsins are upregulated during RIP1-Tag2 tumorigenesis

RIP1-Tag2 transgenic mice develop tumors over time through a series of highly reproducible stages (Hanahan, 1985). To examine the gene expression changes associated with progression through each stage, we performed an Affymetrix microarray profiling experiment on cDNA from pools of normal (nontransgenic) islets, hyperplastic islets, angiogenic islets, and tumors using the 11K and 19K mouse chips (Affymetrix). Following scaling of the hybridization signals for each of the four distinct stages, data sets were grouped using a self-organizing mapping algorithm (SOM) (Tamayo et al., 1999) into clusters of genes showing similar expression patterns (our unpublished data). Several cathepsins were found in a SOM cluster that grouped genes whose expression was low in normal, hyperplastic, and angiogenic islets, and markedly increased in tumors (Figure 1A). Cathepsins H and L were only detectably expressed in tumors, whereas cathepsins C and Z were expressed at much higher levels than in the precursor stages. Two other cathepsins, B and S, were grouped in another cluster that showed a more gradual upregulation during tumorigenesis (Figure 1A). Real-time, quantitative RT-PCR using primer pairs specific for the six cathepsin mRNAs was used to evaluate expression in independently isolated pools of normal islets, angiogenic islets, and tumors. The expression patterns of the six cathepsins in these distinctive stages were similar to those observed in microarray analysis, again indicating upregulation in tumors (our unpublished data).

To determine if the enzymatic activity of these proteases was similarly upregulated during tumorigenesis, we used chemical probes specific for this family of cysteine cathepsins (Greenbaum et al., 2000). These activity-based probes (ABPs) are based on a small molecule scaffold that binds covalently in the active sites of members of the cysteine cathepsin family, thereby allowing their specific identification within cell or tissue lysates. Furthermore, since the probes bind irreversibly to target proteases in an activity-dependent manner, covalent labeling can be used as a direct readout of protease activity levels. Using a biotinylated ABP called DCG-04 (Figure 1B), we detected a progressive increase in overall levels of cathepsin activity during RIP1-Tag2 tumorigenesis (Figure 1C). Individual bands from whole tumor lysates were resolved by 1D gel electrophoresis (data not shown), and identified by single-step purification using the biotin tag, followed by mass spectrometry-based sequencing. Cathepsins B, C, L, and Z (Figure 1C) were identified by their sequence, and their identities confirmed by immunoprecipitation experiments with antibodies recognizing individual cathepsins (data not shown). The specificity of the ABP was confirmed by competition experiments using a broad-spectrum cathepsin cysteine protease inhibitor, JPM-OEt (Meara and Rich, 1996) (Figure 1B), and a cathepsin B-specific inhibitor, MB-074 (Bogyo et al., 1999). Preincubation of tumor lysates with JPM-OEt completely abolished DCG-04 labeling of all active cathepsins in the 20–40 kDa range (lane 2, Figure 1D). Likewise, pretreatment with MB-074 specifically blocked cathepsin B activity (lane 3, Figure 1D; note the absence of the cathepsin B band, as indicated by the asterisk), but not other cathepsins. Heat-inactivated controls also showed that all labeled proteins were in fact proteases (data not shown). We did not detect active cathepsins H or S by mass spectrometric sequencing of proteins purified from whole tumor lysates with DCG-04, which may reflect much lower expression in the case of cathepsin H. However, cathepsin S is expressed at higher levels, both in the whole tumors and in sorted inflammatory cells, and yet it was not detected as an active enzyme in whole tumor lysates. This discrepancy could be attributed to posttranscriptional regulation such that mRNA but not active protease was produced; however, we suspect that the activity probe may bind preferentially to other cathepsins in the complex tumor lysate. Indeed, when the constituent cells were first separated from the whole tumors and lysates labeled with the biotinylated ABP, a band corresponding to the molecular weight of active cathepsin S was detected in the infiltrating immune cells (see Figure 3A, band labeled I*). Ongoing analyses are expected to address this possible explanation.

We next used an ABP to label active proteases in vivo. A cell-permeable fluorescent analog of DCG-04 incorporating the BODIPY fluorophore as a tag, BODIPY 530/550-DCG-04 (Greenbaum et al., 2002) (Figure 1B), was injected intravenously into RIP1-Tag2 mice at different stages of tumor development (Figure 2). There was little or no cathepsin activity detected by the ABP in normal islets (Figures 2A and 2B), nor in the surrounding normal exocrine pancreas, suggesting that the cathepsins expressed in normal lysosomes and secretory granules were either inaccessible to the probe or present at levels below the threshold of detection. In contrast, cathepsin activity was clearly evident in angiogenic islets (Figures 2C and 2D) and tumors (Figures 2E and 2F). The cellular localization of cathepsin activity was further resolved by confocal microscopy, as shown in Figures 2I–2K. Labeled cells within the neoplastic lesions showed either a punctate perinuclear signal (Figures 2I and 2J, arrows) or a diffuse activity localization, suggestive of cell membrane-associated activity, and perhaps of cathepsins secreted into the extracellular microenvironment (Figures 2I and 2K, arrowheads). We are in the process of further defining the subcellular activity colocalization using cell surface and lysosomal markers. Interestingly, there was a clear increase in ca-

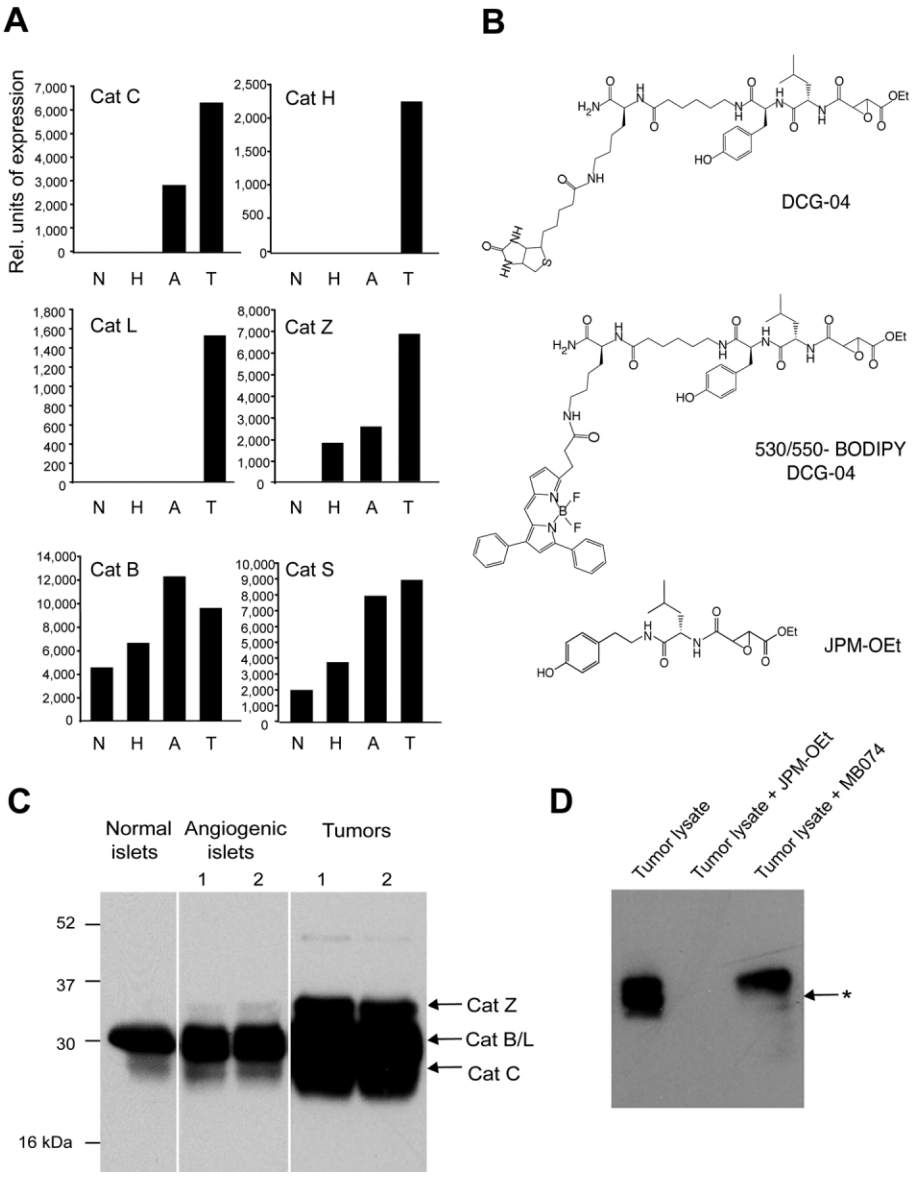

Figure 1. Expression and activity profiling reveals upregulation of a subset of lysosomal cysteine proteases

A: Normalized gene expression values for six cathepsin cysteine proteases from Affymetrix microarrays. Expression values were clustered by self-organizing mapping (SOM), and the first four genes fell into the group (SOM cluster) in which expression was markedly upregulated in tumors compared to the normal case and the premalignant stages. Two of the other cathepsins (cathepsin B and S) represented on the microarray showed a more progressive upregulation. N represents normal islets, H represents hyperplastic islets, A represents angiogenic (dysplastic) islets, and T represents tumors.

B: Molecular structures of small-molecule activity based probes (ABPs) and inhibitors used in this study.

C: Cathepsin activity profiles for progressive stages of RIP1-Tag2 tumor development using the DCG-04 ABP on tissue lysates, controlled for equal loading. Active cathepsin bands positively identified by mass spectrometry sequencing are labeled. Molecular weight markers are indicated on the side panel.

D: Competition experiments on tumor lysates demonstrating specificity of the DCG-04 probe. Incubation of equally loaded tumor lysates with a broad-spectrum inhibitor, JPM-OEt, abolishes activity in the 30–40 kDa range (lane 2), whereas incubation with MB-074, a cathepsin B-specific inhibitor, abolishes cathepsin B activity as indicated by an asterisk (lane 3).

thepsin activity at the invasive edges of the islet carcinomas (Figures 2G and 2H), suggestive of a role in tumor invasion.

Cell type-specific localization of cysteine cathepsin activity

As the islet tumors are comprised of multiple cell types, we sought to identify the cell type(s) responsible for providing cathepsin protease activity. Flow cytometry was used to sort the solid tumors into three constituent cell types (endothelial, innate immune, and tumor) as previously described (Bergers et al., 2003), and ABP profiling of lysates from the purified cell populations was performed using the DCG-04 probe. The labeling of equally loaded samples, consisting of lysates from cell types isolated and purified by flow cytometry, reveals infiltrating innate immune cells to be a significant source of cathepsin activity (Figure 3A). Interestingly, the three constituent cell fractions apparently have distinctive cathepsin activity profiles, as revealed by differential mobility of the probe-labeled proteases by polyacrylamide gel electrophoresis (PAGE). We then used quantitative RT-PCR to identify the individual cathepsin genes expressed in each flow-sorted cell population, as shown in Figure 3B. All six cathepsins were expressed in the infiltrating immune cell fraction, with cathepsins B, C, H, and S being differentially abundant compared to the other cell types. By contrast, the tumor cell fraction preferentially expressed the cathepsin L gene. Two points should be considered when evaluating the relative activity and gene expression profiles in the sorted cell types. First, the endothelial and immune cells represent only 2%–5% of the total cells inside the tumors, with the overt oncogene transformed β cells constituting the majority (~90%–95%), such that the aggregate contribution of protease activity from the overt tumor cells could be comparable to the apparently higher levels in infiltrating immune cells. Second, the in vivo ABP revealed a focal distribution of high-level activity, particularly

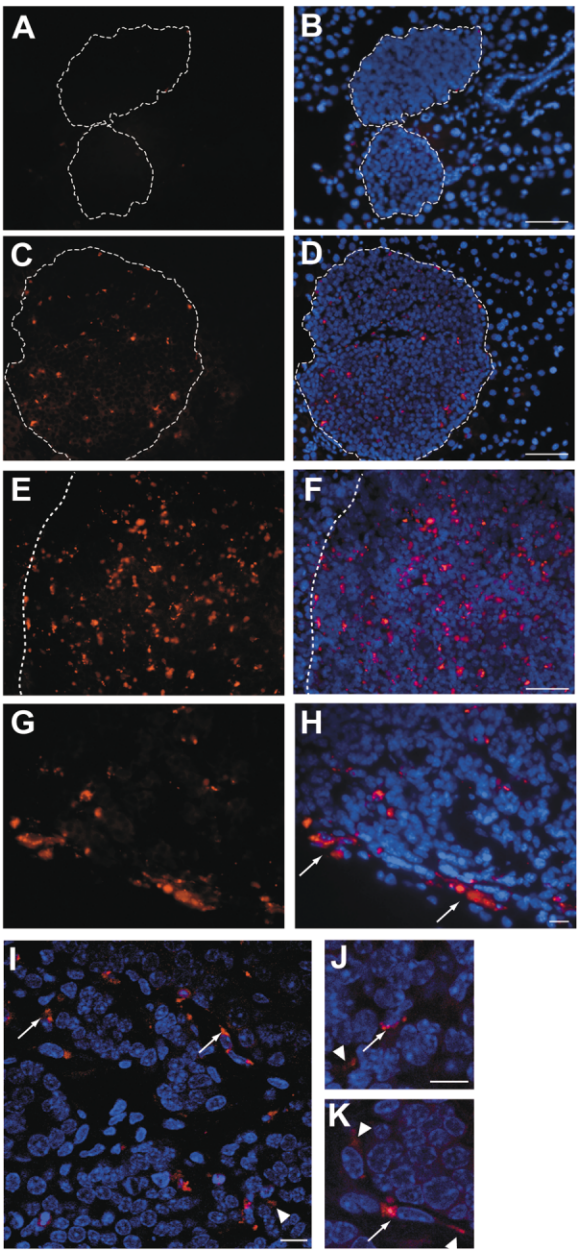

Figure 2. In vivo profiling of cathepsin activity during RIP-Tag tumorigenesis

A–H: Visualization of BODIPY 530/550-tagged DCG-04 in representative images following intravenous injection in RIP1-Tag2 mice. **A** and **B** show the DCG-04 signal and the corresponding DAPI/DCG-04 merged image in normal islets, **C** and **D** in angiogenic islets, **E** and **F** in tumors, and **G** and **H** in invasive tumor fronts. Normal islets and lesions are outlined by the white dotted lines, and surrounded by the normal exocrine pancreas. The scale bar corresponds to 50 μM in **A–F** and 10 μM in **G–H**.

I–K: A subset of cells within RIP1-Tag2 tumors are positive for cathepsin activity, as shown in **I** through **K**. Punctate staining is indicated by arrows, with arrowheads highlighting diffuse staining. The scale bar corresponds to 10 μM in **I** and **J**.

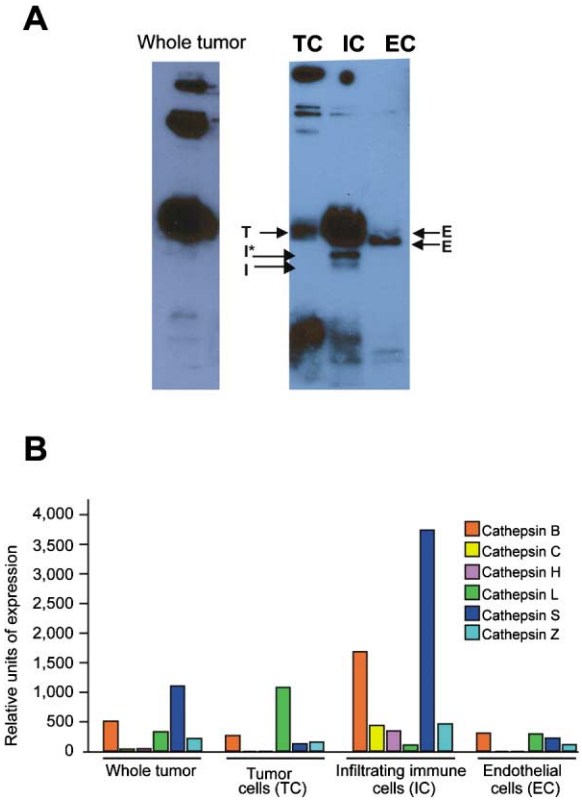

Figure 3. Cell-specific profiles of cathepsin activity and expression in RIP-Tag tumors

A: Different tumor constituent cell types have distinguishing cathepsin activity profiles. RIP1-Tag2 tumors were separated into three constituent cell types by flow cytometry (endothelial [EC], infiltrating immune [IC], and tumor cell [TC] populations), and the cell lysates incubated with DCG-04. The panel on the left corresponds to the activity profile in the presorted whole tumor lysates. Arrows next to the right hand panel indicate cathepsin activities of different molecular weight unique to immune cells (I) and highlight bands differing between tumor (T) and endothelial cells (E). All samples are controlled for equal protein loading.

B: Different constituent cell types in tumors have distinct cathepsin expression profiles. Real-time quantitative RT-PCR of the six cathepsin cysteine proteases, normalized to a mouse housekeeping gene, mGus, was performed on the mRNA of purified cell types isolated from whole tumors by FACS. The highest relative levels of expression were detected in the infiltrating immune cell compartment, with the exception of cathepsin L, which was most abundant in the tumor cell fraction.

associated with the angiogenic vasculature and invasive fronts of carcinomas. These analyses therefore reveal all three cell types to be suppliers of cathepsin activity, but with different biases amongst the six genes; as such, cathepsins produced by each cell type could in principle be playing distinct roles in tumorigenesis.

Inhibition of cathepsin activity affects multiple stages of tumorigenesis

In order to ascertain whether the observed upregulation of cathepsin expression and activity was important for RIP1-Tag2 tumorigenesis, we used a small molecule inhibitor to block protease activity. The E-64d analog JPM-565 (Bogyo et al., 1999; Meara and Rich, 1996; Shi et al., 1992) is a broad-spectrum irreversible inhibitor for the cysteine cathepsin family. The ester analog of JPM-565, where the free carboxylic acid has been replaced with an ethyl ester (termed JPM-OEt), is a cell-permeable analog of JPM-565 (Bogyo et al., 1999) (Figure 1B). This compound was chosen for inhibitor trials due to the increased

likelihood that it would be able to access intracellular as well as extracellular cathepsin targets. RIP1-Tag2 mice were treated with JPM-OEt in three distinctive trial designs that target different stages in tumorigenesis (Bergers et al., 1999). In a 5.5 week prevention trial, designed to assess the effects of a test agent on initial angiogenic switching in the normal vasculature of hyperplastic progenitor lesions, daily injection of JPM-OEt produced a 49% reduction in the number of angiogenic islets evident at a defined endpoint (10.5 weeks of age), when solid tumors are just forming (Figure 4A) (JPM-OEt, $n = 14$, and controls, $n = 20$; $p < 0.0001$). In an intervention trial, designed to interfere with the dramatic growth of nascent solid tumors, JPM-OEt reduced cumulative tumor volume by 67% at 14.5 weeks of age, relative to littermate, sham-treated controls (Figure 4B; $n = 19$, JPM-OEt-treated; $n = 8$, $n = 16$, 11-week and 14.5-week controls respectively; $p < 0.0001$). Finally, in a regression trial, designed to test the ability of inhibitors to stabilize or regress large tumors and modestly extend lifespan to a defined endpoint 4 weeks later, JPM-OEt produced "stable disease," in that the tumor volume at the endpoint was comparable to that in mice at the 12-week-old starting point of the trial (Figure 4B). Untreated RIP1-Tag2 mice die at 13–15 weeks of age; hence there were no age-matched controls for the JPM-OEt mice treated for 4 weeks to the defined endpoint. Therefore, we compared the tumor volumes in 14.5-week-old controls with 16-week-old JPM-OEt-treated mice, revealing a 63% reduction ($p < 0.0001$).

To confirm that the effects of JPM-OEt could be specifically attributed to inhibition of cysteine cathepsins, we used the cysteine cathepsin-specific ABPs to assess the inhibition of cathepsin activity in tumors of mice treated with JPM-OEt; treated tumors were analyzed both by ex vivo and in vivo labeling, as shown in Figures 4C–4E. Tumor lysates from mice treated with JPM-OEt (collected six hours after the final injection of JPM-OEt) versus control littermate tumors showed a marked reduction in cathepsin activity (Figure 4C, 70%–80%, using NIH Image software) as measured by residual labeling with the DCG-04 probe. Similarly, cathepsin activity in vivo was also dramatically reduced, as shown for representative images in Figures 4D and 4E in which RIP1-Tag2 mice treated with JPM-OEt (Figure 4D) are compared to control littermates (Figure 4E) injected under identical conditions with the fluorescent DCG-04 probe. It is notable that the daily inoculation of mice with JPM-OEt had no discernable toxic side effects, even after treating mice for 5.5 weeks. Thus, we observed a clear therapeutic window, in that all three experimental therapeutic trials demonstrated anti-tumor efficacy without evident toxicity.

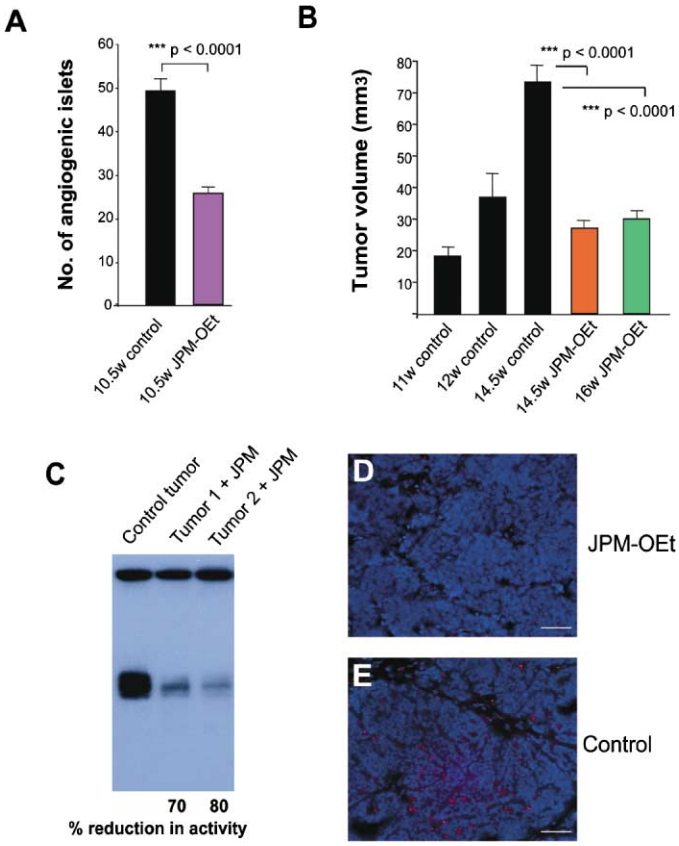

Figure 4. Inhibition of cathepsin activity affects multiple stages of RIP1-Tag2 tumor development

A: Inhibition of cathepsin activity by JPM-OEt significantly decreases the number of angiogenic islets (by 49%) in RIP1-Tag2 10.5-week-old mice ($n = 20$ controls, $n = 14$ JPM treated, ***$p < 0.0001$). The means + SEM (Wilcoxon test) are indicated.

B: Inhibition of cathepsin activity significantly reduces tumor burden in RIP1-Tag2 mice ($n = 8$, $n = 8$, $n = 19$, for 11-week, 12-week, and 14.5-week RIP1-Tag2 controls, respectively. $n = 16$, and $n = 14$ for JPM-OEt-treated 14.5- and 16-week-old mice). The tumor burden in 14.5-week JPM-OEt treated mice is reduced by 67% compared to age-matched untreated controls (***$p < 0.0001$). There are no age-matched control comparisons for the 16-week JPM-OEt treated mice, and thus the comparison was made to 14.5-week controls, which was statistically significant (***$p < 0.0001$, 63% reduction). The means + SEM (Wilcoxon test) are indicated.

C: Cathepsin activity is diminished following treatment of RIP1-Tag2 mice with a broad-spectrum cathepsin inhibitor, JPM-OEt. Tumor lysates from multiple JPM-OEt-treated animals and controls were incubated with DCG-04 in vitro, and gel analysis on equally loaded samples indicates a significant decrease in residual cathepsin activity in tumor lysates (70%–80% reduction as assessed by NIH Image software).

D–E: Cathepsin activity in vivo revealed by the fluorescent ABP is also greatly reduced following JPM-OEt treatment. **D** shows the inhibition of cathepsin activity by JPM-OEt as compared to untreated control littermates (**E**). Scale bar: 50 μM.

Cathepsin activity contributes to angiogenic switching, tumor vascularity, and proliferation

We then investigated the mechanism responsible for the substantive reduction in both angiogenic switching and tumor volume in JPM-treated mice. The vascularity in angiogenic islets and tumors was assessed by perfusion of a fluorescent-labeled lectin through the circulatory system. JPM-OEt-treated angiogenic islets did not show any obvious differences in vascularization, as visualized by the FITC-lectin, compared to control 10.5-week angiogenic lesions (Figures 5A and 5B). Thus, much like analogous studies with an MMP inhibitor and MMP-9 gene knockout mice (Bergers et al., 2000), fewer hyperplastic islet progenitors switched on angiogenesis, but those that did were indistinguishable, indicative of alternative pathways to the same angiogenic premalignant state. In contrast, many of the JPM-OEt-treated tumors showed a pronounced reduction in vessel density, particularly in the core of larger tumors (Figure 5D), as compared to the highly vascularized control tumors (Figure 5C). We confirmed the reductions in vascularity by immunostaining with two endothelial-selective antibodies, CD31 and MECA32, and observed similar results (data not shown). The particular

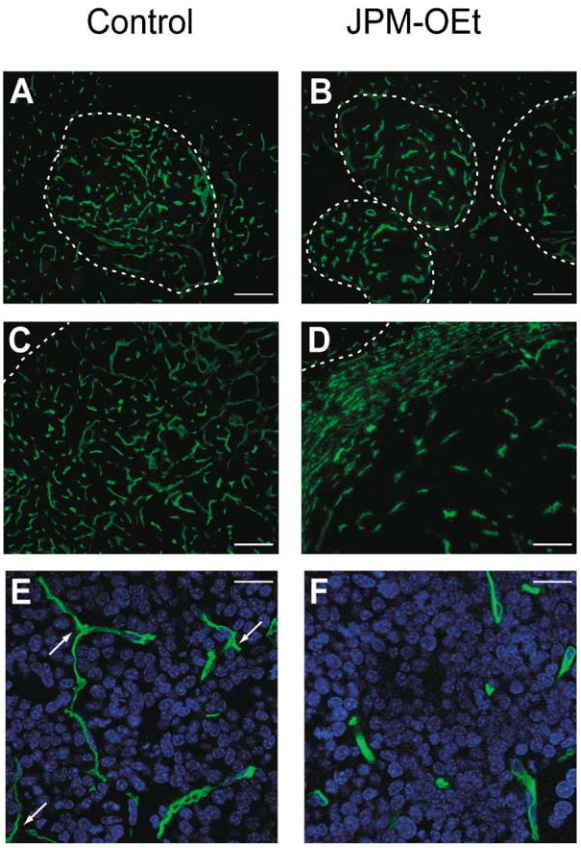

Figure 5. Inhibition of cathepsin activity affects tumor vascularization during RIP1-Tag2 tumorigenesis

A–F: Perfusion of RIP1-Tag2 control (**A**) and JPM-OEt-treated mice (**B**) with FITC-lectin revealed no obvious changes in the vasculature of angiogenic islets at 10.5 weeks of age. However, there were significant reductions in vascularity seen in solid tumors, as shown by representative comparisons in **C** versus **D**, in which the tumor core vasculature was particularly affected. Islets are outlined by dashed white lines, and tumor margins are similarly indicated, with normal exocrine tissue shown in the top left-hand corners. Vascular branching is also affected in JPM-OEt-treated tumors (**F**) in which branchpoints (indicated by arrowheads in the control tumor [**E**]) are greatly reduced or absent, in representative images. The scale bar corresponds to 50 μM in **A–D** and 25 μM in **E** and **F**.

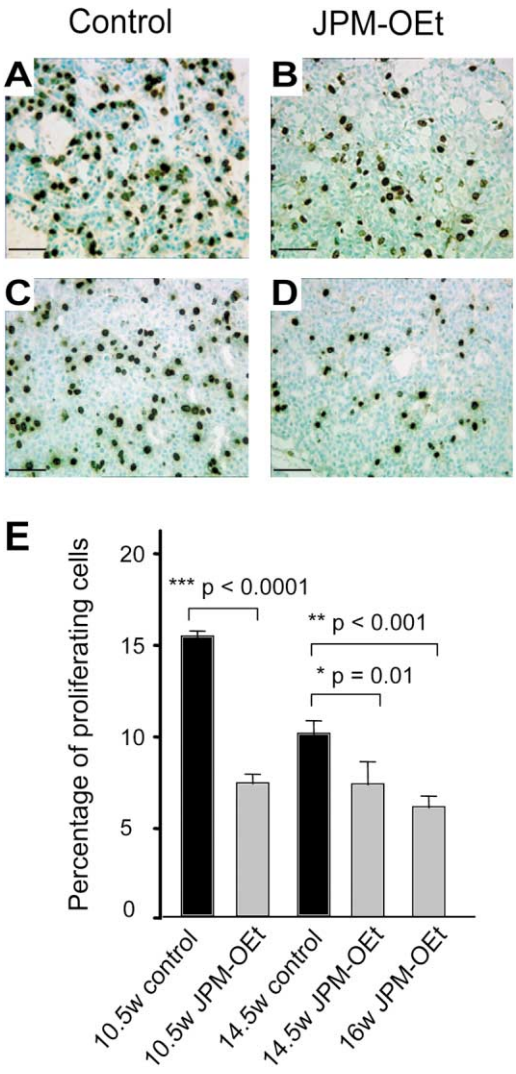

Figure 6. Cell proliferation is reduced following cysteine cathepsin inhibition

A–D: Proliferating cells were detected by BrdU incorporation and representative images are shown for 10.5-week control (**A**), JPM-OEt (**B**), 14.5-week control (**C**), and JPM-OEt (**D**) treated time points. Scale bar: 50 μM.

E: Graph showing the relative percentages of proliferating (BrdU positive) cells in treated versus control mice from the three different JPM-OEt trials. The reduction in proliferating cells by comparison to the relevant controls are 52%, 28%, and 39%, respectively, for JPM-OEt-treated 10.5-, 14.5-, and 16-week-old mice. The means + SEM. (Wilcoxon test) are indicated.

defect in vascularization of the core, but not the edges of JPM-OEt-treated tumors, may reflect vessel cooption at the tumor margins from the surrounding normal, exocrine tissue (Holash et al., 1999).

The tumor vasculature was also characterized by a reduction of vessel branching in JPM-OEt-treated versus untreated tumors (Figures 5E and 5F), suggesting impairment of endothelial basement membrane degradation as a result of inhibiting cathepsin activity. It is well established that proteolysis of the basement membrane is a critical step in vessel sprouting during angiogenesis (Carmeliet, 2003; Kalluri, 2003), and interestingly, cathepsin B has been shown to directly degrade three major basement membrane components, laminin, collagen IV, and fibronectin, at physiological pH (Buck et al., 1992). It is also notable that a recent study of a cathepsin S knockout mouse implicated cathepsin S as an enhancer of angiogenesis associated with wound healing in the skin (Shi et al., 2003), suggesting that it in particular may be involved in the angiogenic component of the effects we attribute to cathepsin activity in pancreatic islet tumorigenesis.

Tumor cell proliferation, as assessed by BrdU incorporation, was significantly decreased in all stages of RIP1-Tag2 tumorigenesis, particularly in the angiogenic islet stage (Figures 6A–6D). There was a 52% reduction in cell proliferation in JPM-OEt-treated angiogenic islets ($p < 0.0001$), while proliferation in JPM-OEt-treated tumors was reduced by 28% in 14.5-week mice (I.T.) ($p = 0.01$) and 39% in 16-week mice (R.T.) ($p < 0.001$), as compared to 14.5-week controls (Figure 6E). Since the vasculature in the angiogenic islets of JPM-OEt-treated mice was indistinguishable from that of controls (albeit less frequent), the reduced proliferation index suggests that JPM-OEt is di-

rectly interfering with tumor cell growth. Thus we imagine a direct role for cysteine cathepsins in facilitating proliferation of the oncogene-expressing β cells, in addition to effecting a robust tumor vasculature.

In contrast to the effects on cell proliferation, inhibition of cathepsin activity with JPM-OEt had no discernible impact on the frequency of apoptosis (data not shown). While certain cathepsins have been shown to be involved in mediating apoptosis triggered by specific stimuli (e.g., TNF-induced apoptosis [Foghsgaard et al., 2001]), the pharmacological trials with JPM-OEt indicate that cathepsins are not centrally involved in the acquired resistance to apoptosis that is demonstrably important in this islet tumorigenesis model (Christofori et al., 1994; Naik et al., 1996).

Cathepsins contribute to the capability for invasive growth

The in vivo ABP revealed a focal increase in cathepsin activity at the invasive edges of tumors (Figures 2G and 2H), suggesting a role in facilitating local tumor invasion. Consistent with this hypothesis, daily treatment of RIP1-Tag2 mice with JPM-OEt significantly delayed progression to both widely invasive (IC-2) and microinvasive (IC-1) carcinomas in both intervention (I.T.) and regression trials (R.T.) (Figure 7G). Detailed grading of hematoxylin and eosin-stained tumors (Lopez and Hanahan, 2002) showed that mice treated in an intervention trial with JPM-OEt had no high-grade IC-2 class carcinomas, producing a clear and significant shift toward more benign, encapsulated tumors (representative images shown in Figures 7A and 7B). When starting the treatment regimen later, in a regression trial at 12 weeks (where carcinomas have already formed), JPM-OEt significantly reduced but did not abolish the incidence of invasive tumors of both classes at 16 weeks. Since the epithelial cell-cell interaction molecule E-cadherin is characteristically downregulated upon progression to carcinomas (Perl et al., 1998; Vleminckx et al., 1991), in particular in the RIP1-Tag2 model, we used it as an independent criterion for the invasive growth capability, to complement the grading of H&E stained sections; to that end, tumors from JPM-OEt-treated and control RIP1-Tag2 mice were immunostained with antibodies for E-cadherin. There was a complete concordance with the histological grading of invasion: we detected no tumors that lacked E-cadherin expression altogether (IC-2) following an I.T., and saw reduced frequencies of tumors with uniform or localized downregulation of E-cadherin (IC-2 and IC-1, respectively) after the R.T. (representative images shown in Figures 7C–7F). Thus, by both criteria, cathepsin activity is contributing to the invasive growth program, as evidenced by suppression of invasive carcinomas with the JPM-OEt inhibitor, consistent with the in situ labeling by the ABP of cathepsin activity in invasive regions of the tumors (Figures 2G and 2H).

Cysteine cathepsin activity is upregulated during tumor development in a mouse model of cervical cancer

To begin addressing the general relevance of the pronounced upregulation in cysteine cathepsin expression and activity observed in the RIP1-Tag2 model of islet cell carcinogenesis, we have used the fluorescent ABP to visualize in vivo activity in another mouse model of human cervical cancer. These transgenic mice express the human papillomavirus type 16 oncogenes under the keratin 14 promoter and develop invasive can-

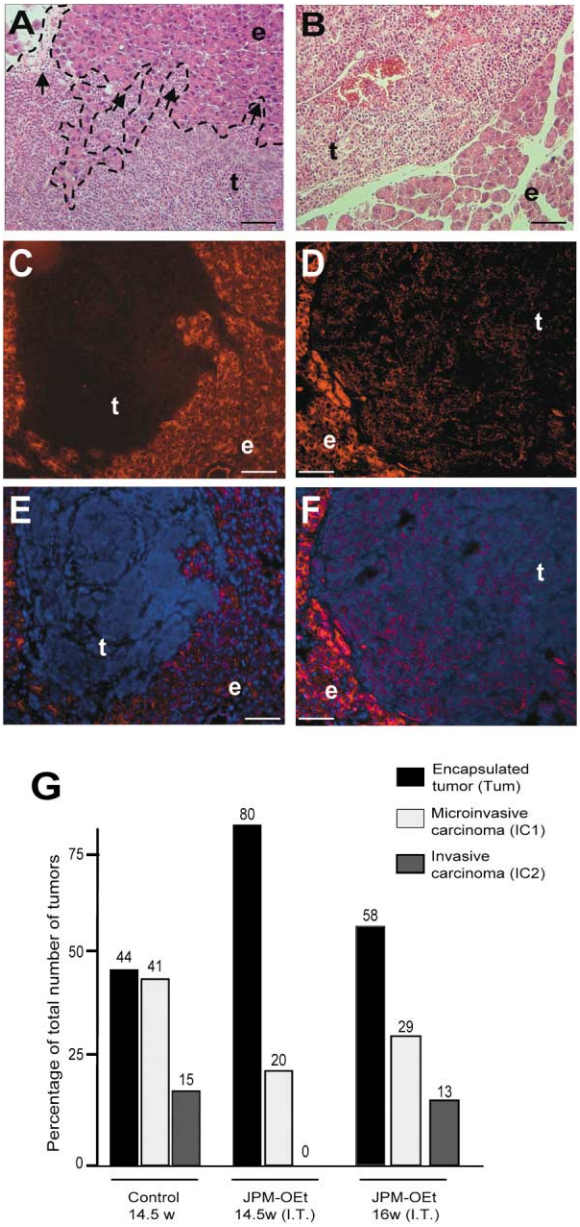

Figure 7. Inhibition of cathepsin activity reduces invasive properties of RIP1-Tag2 tumors

A and B: Histological comparison of representative 14.5-week control (**A**) and JPM-OEt-treated (**B**) tumors. Multiple invasive fronts are frequent in control tumors as indicated by arrows, whereas the majority of JPM-OEt-treated tumors (t) remain encapsulated and histologically distinct from the surrounding normal exocrine tissue (e). Scale bar: 50 μM.

C–F: E-cadherin downregulation, diagnostic of the invasive phenotype, is not evident in JPM-OEt-treated tumors (**D** and **F**) as compared to control tumors (**C** and **E**). E-cadherin immunostaining is shown in red (**C** and **D**) and merged with the DAPI counterstain (**E** and **F**). t indicates tumor, and e indicates normal exocrine pancreas. Scale bar: 100 μM.

G: Graph showing the relative proportions of encapsulated, microinvasive, and invasive carcinomas in controls versus 14.5-week JPM-OEt, and 16-week JPM-OEt (R.T.) -treated mice, revealing fewer malignant tumors following JPM-OEt treatment. Comparison of the two time points is indicative of delayed time to progression to carcinoma, a parameter commonly used to evaluate responses in human clinical trials.

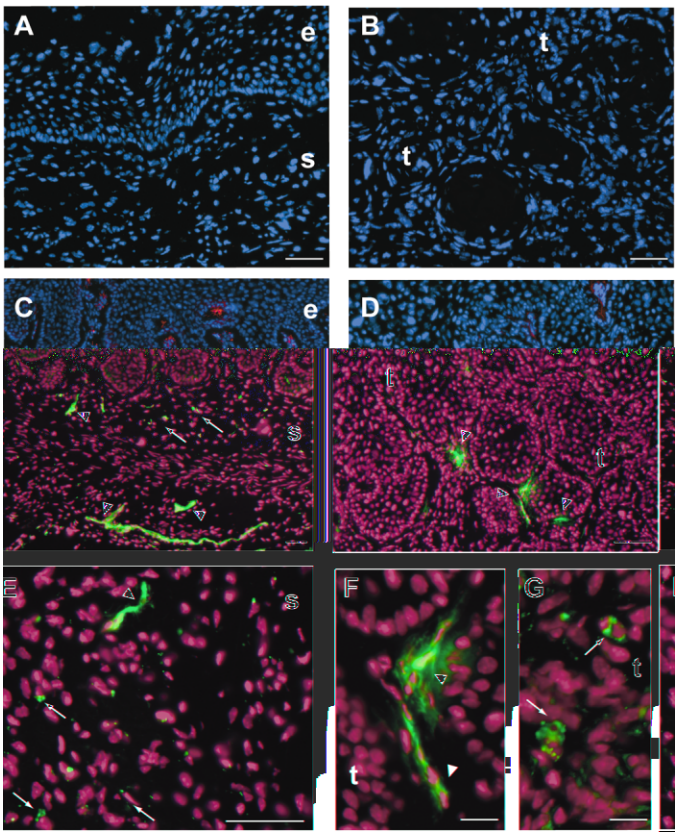

Figure 8. In vivo imaging with the activity-based probe reveals cathepsins are also activated during HPV16-induced cervical carcinogenesis

Representative images are shown following intravenous injection of the fluorescent ABP (BODIPY530/550-tagged DCG-04) into multiple K14-HPV16/E_2 and control mice; cervical tissue sections were stained with DAPI and visualized by fluorescent microscopy.

A: The cervix in an estrogen-treated FVB/n control mouse did not evidence cathepsin activity, either in the epidermis (e) or underlying stroma (s).

B: A cervical tumor (t) in a K14-HPV16/E_2 transgenic mouse injected with a mock solution (PBS) did not have a background autofluorescent signal.

C: A K14-HPV16/E2 mouse with high-grade cervical dysplasia (CIN-3) had cathepsin activity throughout the underlying stroma (s) below the CIN-3 lesion (e), both in a punctate manner (arrows) as well as in angiogenic blood vessels (arrowheads).

D: A similar localization of cathepsin activity was seen in stroma adjacent to the invasive fronds of a cervical carcinoma (t).

E–G: Higher magnification of a dysplastic lesion (**E**) reveals both cell-associated punctate activity and colocalization with the angiogenic vasculature, as is also the case in tumors (**F** and **G**, respectively). The scale bar corresponds to 50 μM in **A–E** and 25 μM in **F–G**.

cers in the context of sustained estrogen levels (K14-HPV/E_2) via a series of lesional stages analogous to those in humans (Arbeit et al., 1996; Elson et al., 2000). The K14-HPV/E_2 mice evidence a similar angiogenic switch to that observed in RIP1-Tag2 mice and in the human cervix (Smith-McCune et al., 1997), with intense angiogenesis underlying advanced dysplasias (CIN 3) and invasive carcinomas. No cysteine cathepsin activity was detected in the normal cervix of control female mice (FVB/n/E_2) following intravenous injection of the fluorescent cysteine cathepsin ABP (Figure 8A). In contrast, K14-HPV/E_2 mice bearing CIN-3 dysplasias or tumors revealed significant levels of cysteine cathepsin activity. In the CIN-3 lesions, activity was localized to the stroma underlying the dysplastic epidermis (Figure 8C), and was seen throughout the cervical tumors (Figure 8D). Higher magnification of both the dysplastic (Figure 8E) and cancerous (Figures 8F and 8G) lesions revealed a similar activity localization to that seen in the lesional pancreas of RIP1-Tag2 mice, associated both with the cell surface of endothelial cells (Figure 8F) and with punctate perinuclear regions of individual cells within the tumor (Figure 8G).

Discussion

In this study, activity-based probes and a class-specific small molecule inhibitor were used to investigate the functional importance of the cathepsin cysteine proteases in cancer. We found that several cathepsins were upregulated during tumor progression and then demonstrated their functional involvement in a prototypical mouse model of pancreatic islet cell cancer. Of the eleven known mammalian cysteine cathepsins (Turk et al., 2002), expression of six mouse cathepsin genes was upregulated during RIP1-Tag2 tumorigenesis. Four of these cathepsins (B, C, L, and Z) were specifically identified as being substantively increased in their protease activity in solid tumors. The potential of reporter substrates to probe protease activity in tumors in vivo has previously been demonstrated (Bremer et al., 2001; Tung et al., 2000) using xenografts of human cancer cell lines that expressed high levels of the candidate proteases. While illustrative, the experimental design did not allow for evaluation of the endogenous proteases within a tumor or its constituent cell types. Furthermore, this method does not allow for the biochemical analysis of target proteases contributing to hydrolysis of the reporter. We have expanded and refined this approach, showing herein that ABPs for cathepsin cysteine proteases can be used to visualize endogenous protease activity in vivo during the stepwise progression of organ-specific tumorigenesis, and we demonstrate that the proteases involved can be identified and monitored biochemically.

Our use of a small-molecule inhibitor to pharmacologically knock out protein function has revealed roles for cysteine cathepsins during initial angiogenic switching in hyperplastic and dysplastic islet progenitor lesions, as well as for tumor growth, tumor vascularity, and invasion. The delay in and reduced frequency of progression to invasive carcinoma when the cathepsin cysteine proteases are inhibited is of particular interest. Cathepsins have been proposed to function in the initiating steps of a proteolytic cascade involving serine proteases and MMPs (reviewed in Koblinski et al., 2000; Rao, 2003). However, both individual gene knockouts of members of the MMP and serine protease family (MMP-2, MMP-9 and uPA) and broad-spectrum MMP inhibition did not affect progression to invasive carcinomas in this model (Bergers et al., 2000). We propose, therefore, that the cathepsins are facilitating the invasive growth capability, a hallmark of malignancy, through a distinctive pathway. One attractive mechanism would involve proteolysis of E-cadherin, given that loss of E-cadherin function is a determinant of the invasive growth capability in this (Perl et al., 1998) and other tumors (Strathdee, 2002; Vleminckx et al., 1991), and that extracellular proteolysis has been implicated as one means to abolish its function (Ito et al., 1999; Rios-Doria et al., 2003); this possibility is the subject of ongoing investigation.

Evaluation of the constituent cell types purified from tumors by flow cytometry (using both quantitative RT-PCR and ABPs)

revealed that the candidate cathepsin genes were most prominently expressed in innate immune cell types (granulocytes and macrophages), as well as in endothelial and tumor cells. Three of the six genes were expressed in all three cell fractions, while cathepsins C and H were selectively expressed by immune cells, and cathepsin L was preferentially expressed in the tumor cell compartment. This multiplicity of sources for cathepsin activity is provocative: perhaps different cell types are contributing cathepsins required to manifest distinct functions among the set we have attributed by their collective pharmacological inhibition. The prominence of expression of the implicated cathepsin genes by innate immune cells adds further weight to the growing consensus that immune infiltrates have the potential to be tumor-enhancing (Coussens and Werb, 2002). Indeed, we have previously shown that MMP-9, a matrix metalloprotease, is supplied exclusively by infiltrating innate immune cells in the RIP1-Tag2 model (Bergers et al., 2000, and our unpublished observations), where it is principally involved in mobilizing VEGF-A during the initial angiogenic switch in progenitor lesions (Bergers et al., 2000). Cysteine cathepsins, in contrast, are supplied by multiple constituent cell types within islet tumors, and have a crucial, nonoverlapping function to that of the MMPs, in facilitating progression to the invasive carcinoma stage.

Taken together, the data raise important questions for the future. Which individual cathepsin genes are important for the various ascribable functions during tumorigenesis? What cell type(s) contributes the necessary activity for each of these capabilities? Both cathepsin gene knockout mice and cathepsin subtype-selective inhibitors should provide avenues to address these questions. A broader issue is the prevalence of cathepsin upregulation in other types of cancer, a question we have begun to evaluate in another mouse model of cancer, the K14-HPV/E_2 model of cervical carcinoma. Interestingly, we observed a similar induction of cysteine cathepsin activity that was not evident in the normal cervix, by using the in vivo ABP. Cathepsin activity appeared concomitant with the angiogenic switch in the dysplastic lesions and was maintained in tumors, much as we had observed in the RIP1-Tag2 model. Future functional studies in this and other models should provide insight into the general involvement of cysteine cathepsins in tumor development in other organs.

If one accepts that our prototypical mouse model may have predictive value for human clinical trials, the lack of apparent toxicity and the demonstrable efficacy of the JPM-OEt inhibitor when used to target both early and late stages of islet tumorigenesis are encouraging. Although many human cancers express high levels of cathepsin activity, to date, these proteases have not been prominent drug candidates, likely because of limited data implicating them in a direct involvement in tumor progression. However, one note of caution when considering pharmacological inhibitors of cysteine cathepsins relates to the endogenous inhibitors of cathepsin activity, the cystatins (Turk et al., 2002). Although their function is broadly antitumorigenic (Konduri et al., 2002; Rao, 2003), there have been recent reports that certain cystatins are prometastatic in some experimental systems (Huh et al., 1999; Morita et al., 1999; Utsunomiya et al., 2002), inferring that particular cathepsins could be antimetastatic. However, there are indications that cystatins have novel functions independent of their role as cysteine cathepsin inhibitors (Shridhar et al., 2003). These cathepsin-independent functions may, or may not, be contributing to the complex tumor-modulatory responses attributed to the cystatins in other experimental systems. In any event, the cystatins warrant consideration along with the cathepsins as factors influencing tumor phenotypes in mouse models and in human cancers.

In conclusion, with the evidence presented here, perhaps cysteine cathepsin inhibitors such as JPM-OEt (which shows efficacy and no apparent toxicity in the trials performed in this mouse model), or vinyl sulfone peptidomimetics (e.g., N-methyl piperazine-Phe-hPhe-vinyl sulfone phenyl, which is entering clinical trials for Chagas disease [Engel et al., 1998; McKerrow et al., 1999]), should be considered for clinical trials treating cancers known to upregulate these proteases. It is reasonable to suggest that cathepsin inhibitors may show combinatorial benefits with other targeted (and traditional) therapies, which could be revealed in preclinical trials involving this and other mouse models of human cancer.

Experimental procedures

Transgenic mice breeding

The generation of RIP1-Tag2 mice as a model of pancreatic islet cell carcinogenesis has been previously reported (Hanahan, 1985). Similarly, the generation of K14-HPV16 transgenic mice (Coussens et al., 1996) and their treatment with 17β-estradiol (E_2) for cervical carcinogenesis has been reported (Arbeit et al., 1996; Elson et al., 2000). Mice were maintained in accordance with the University of California, San Francisco (UCSF) institutional guidelines governing the care of laboratory mice.

Microarray and real-time quantitative PCR

Normal (nontransgenic BL/6) and hyperplastic islets (from 5-week-old RIP1-Tag2 mice) were collected as previously described (Parangi et al., 1995). Angiogenic islets were isolated from 8-week-old RIP1-Tag2 mice by collagenase digestion of the excised pancreas, and selected based on their red, hemorrhagic appearance (Parangi et al., 1995). Tumors were microdissected from the excised pancreas of 13-week-old RIP1-Tag2 mice and the surrounding exocrine tissue carefully removed. RNA was prepared from pools of snap-frozen islets and tumors using an RNeasy kit (Qiagen), DNase treated, and LiCl precipitated. 10 μg of total RNA was used in cDNA synthesis, and labeled cRNA subsequently generated using standard protocols. Microarray hybridizations to the mouse 11K and 19K chips and measurement of hybridization intensities were carried out according to manufacturer's protocols (Affymetrix Inc). Each data set was rescaled to normalize for differences of microarray intensities across the different sets. This scaled data was then analyzed using self-organizing map (SOM) (Tamayo et al., 1999) analysis to cluster genes with similar expression profiles. Real-time quantitative RT-PCR was performed on cDNA synthesized from normal, angiogenic islets and tumors, or flow-sorted cells using the 5′ nuclease assay (real-time TaqMan RT-PCR) with the ABI PRISM 7700 instrument (ABI) as previously described (Elson et al., 2001). Gene-specific primers and probes were designed for six cathepsins; cathepsin B (forward primer: 5′-TTTGATGCACGG GAACAATG-3′ and reverse primer: 5′-TTGGTGTGAATGCAGGTTCG-3′, probe: CGGCTCTTGTTGGGCATTTGGG), cathepsin C (forward: 5′-AAA TGAGCCTGCGAGATCTGA-3′ and reverse: 5′-ATTGACGCCTTGGACGT TTC-3′, probe: AAGGATCCCAAGGCCCAAACCTGC), cathepsin H (forward: 5′-GATGTATAAAAGTGGCGTCTACTCCA-3′ and reverse: 5′-GTTCAATG AGGAAGTACCCATTCTC-3′, probe: CCTGGCGGTTGGCTATGGAGAA CAG), cathepsin L (forward: 5′-AATACAGCAACGGGCAGCA-3′ and reverse: 5′-AGCGGTTCCTGAAAAAGCCT-3′, probe: CGCCTTTGGTGACATGACCA ATGAGG), cathepsin S (forward: 5′- CGCCAGCCATTCCTCCTT-3′, reverse: 5′-ATGATTCACATTGCCCGTACAG-3′, probe: ACAAAAGCGGTGTCTATG ACGACCCC), cathepsin Z (forward: 5′-CCTGTCCGGGAGGGAGAA-3′ and reverse 5′-TGGTTGATAACGGCCTGGTC-3′, probe: TCCCATCAGCTGCG GGATAATGG).

Preparation and labeling of tissue lysates

Normal islets, angiogenic islets, and tumors were collected as above and homogenized in lysis buffer (5 mM acetate [pH 5.5], 1 mM EDTA, 2 mM DTT, 0.1% Triton X-100), and protein concentrations quantitated using the

Bradford assay. The lysates were labeled with DCG-04 and equally loaded and analyzed by gel electrophoresis as previously described (Greenbaum et al., 2000). Equal numbers of flow-sorted RIP1-Tag2 tumor cells were similarly labeled and analyzed.

In vivo labeling and detection

RIP1-Tag2 mice at different ages (8 weeks and 13 weeks) and control C57Bl/6J mice were anesthetized with an intraperitoneal injection of 2.5% avertin. Mice were individually weighed and BODIPY530/550-DCG-04 (1 mM solution in 10 mM HEPES [pH 7.4]; 10% DMSO w/v) was intravenously injected through the tail vein (volume to be injected in μl = 5$\times$ mouse weight in grams, i.e., 150 μl for a 30 g mouse) and allowed to circulate for 1–2 hr, followed by heart perfusion with PBS and then formalin. The pancreas was excised and fixed in formalin for 1 hr, rinsed in PBS, and immersed in 30% sucrose, followed by embedding in OCT compound. Frozen sections were cut at 10 μm thickness, rinsed in PBS, and covered with Vectashield with DAPI (Vector) to visualize nuclei. At least five mice per age group were analyzed. K14-HPV/E2 mice were similarly analyzed at two different stages: when they typically have CIN-3 dysplasia (5 months of age) or tumors (7 months of age). FVB/n mice treated with estrogen were used as controls and three mice per group (control, dysplasia, and tumor-bearing) were injected with the BODIPY ABP as detailed above, and the cervix was removed and processed as above.

Flow cytometry

Tumors were excised from 13- to 14-week-old RIP1-Tag2 mice and inflammatory, endothelial, and tumor cells collected as previously described (Bergers et al., 2003).

Synthesis of activity-based probes and inhibitors

The activity-based probe DCG-04 and the inhibitor JPM-OEt were synthesized as described (Bogyo et al., 1999; Greenbaum et al., 2000; Meara and Rich, 1996).

Pharmacological trials of the JPM cathepsin inhibitors

The dosing regimen for the three different RIP1-Tag2 trials was determined by injection of various concentrations of JPM-OEt (10, 25, 50, or 100 mg/kg/day) for 5 days, followed by injection of the BODIPY530/550-DCG-04 probe and PAGE analysis to assess the reductions in protease activity (unpublished data). 50 mg/kg/day as a single daily intraperitoneal injection was determined to be the optimal dose and used for all in vivo studies, and JPM-OEt was administered in 30% DMSO/70% PBS. Independent trials were performed at least twice on groups containing equal numbers of male and female RIP1-Tag2 mice. Control littermates were treated with 30% DMSO/70% PBS. All in vitro and in vivo analysis of cathepsin activity using the ABPs was performed 6 hr after the final injection of JPM-OEt. Tumor volume and angiogenic islet quantitation were performed as previously described (Bergers et al., 1999; Inoue et al., 2002), and the Wilcoxon t test was used for statistical analyses and calculation of means and SEM. All animal studies were performed using protocols approved by the animal care and utilization committee at the University of California at San Francisco.

Tissue preparation and immunohistochemistry

Tissues were prepared as previously described for frozen and paraffin embedding (Lopez and Hanahan, 2002). FITC-lectin (Inoue et al., 2002) BrdU, TUNEL and E-cadherin staining, and H&E grading (Lopez and Hanahan, 2002) were performed as previously described. For BrdU and TUNEL quantitation, at least 5 graded lesions per mouse (typically 10–15), and at least 5 mice per age-matched group were counted blindly, subsequently decoded, and statistical analysis performed. For grading of tumors, paraffin or frozen tissue blocks were sectioned completely, and tissue sections were stained by H&E every 50 μM, and all tumors in all treated and control RIP1-Tag2 mice were graded.

Acknowledgments

We thank C. Concengco and K. Gilliland for excellent technical assistance, D. Ginzinger and M. Yu, UCSF Cancer Center Genome Facility, for Taqman analysis, A. McMillan for statistical advice, and Bill Bowes for support and encouragement. We gratefully acknowledge L. Lanier, J. McKerrow, K. Shannon, and Z. Werb for helpful and insightful suggestions to the manuscript. This research was supported by the Leukemia and Lymphoma Society (J.A.J.), the William K. Bowes, Jr. Foundation (J.A.J., N.M.M., E.G., J.H.H., and D.H.), grants from the U.S. National Cancer Institute (J.A.J., N.M.M., E.G., J.H.H., and D.H.), the Sandler Family Program in Basic Sciences (A.B., K.C., and M.B), and a subcontract from a U.S. Department of Defense Breast Cancer Center of Excellence Award (BCCOE) DAMD-17-02-1-0693 (M.B.).

Received: January 23, 2004
Revised: March 6, 2004
Accepted: March 17, 2004
Published: May 17, 2004

References

Arbeit, J.M., Howley, P.M., and Hanahan, D. (1996). Chronic estrogen-induced cervical and vaginal squamous carcinogenesis in human papillomavirus type 16 transgenic mice. Proc. Natl. Acad. Sci. USA *93*, 2930–2935.

Balaji, K.N., Schaschke, N., Machleidt, W., Catalfamo, M., and Henkart, P.A. (2002). Surface cathepsin B protects cytotoxic lymphocytes from self-destruction after degranulation. J. Exp. Med. *196*, 493–503.

Bergers, G., Javaherian, K., Lo, K.M., Folkman, J., and Hanahan, D. (1999). Effects of angiogenesis inhibitors on multistage carcinogenesis in mice. Science *284*, 808–812.

Bergers, G., Brekken, R., McMahon, G., Vu, T.H., Itoh, T., Tamaki, K., Tanzawa, K., Thorpe, P., Itohara, S., Werb, Z., and Hanahan, D. (2000). Matrix metalloproteinase-9 triggers the angiogenic switch during carcinogenesis. Nat. Cell Biol. *2*, 737–744.

Bergers, G., Song, S., Meyer-Morse, N., Bergsland, E., and Hanahan, D. (2003). Benefits of targeting both pericytes and endothelial cells in the tumor vasculature with kinase inhibitors. J. Clin. Invest. *111*, 1287–1295.

Bogyo, M., Verhelst, S., Bellingard-Dubouchaud, V., Toba, S., and Greenbaum, D. (1999). Selective targeting of lysosomal cysteine proteases with radiolabeled electrophilic substrate analogs. Chem. Biol. *7*, 27–38.

Bremer, C., Tung, C.H., and Weissleder, R. (2001). In vivo molecular target assessment of matrix metalloproteinase inhibition. Nat. Med. *7*, 743–748.

Brix, K., Linke, M., Tepel, C., and Herzog, V. (2001). Cysteine proteinases mediate extracellular prohormone processing in the thyroid. Biol. Chem. *382*, 717–725.

Buck, M.R., Karustis, D.G., Day, N.A., Honn, K.V., and Sloane, B.F. (1992). Degradation of extracellular-matrix proteins by human cathepsin B from normal and tumour tissues. Biochem. J. *282*, 273–278.

Carmeliet, P. (2003). Angiogenesis in health and disease. Nat. Med. *9*, 653–660.

Christofori, G., Naik, P., and Hanahan, D. (1994). A second signal supplied by insulin-like growth factor II in oncogene-induced tumorigenesis. Nature *369*, 414–418.

Coussens, L.M., and Werb, Z. (2002). Inflammation and cancer. Nature *420*, 860–867.

Coussens, L.M., Hanahan, D., and Arbeit, J.M. (1996). Genetic predisposition and parameters of malignant progression in K14–HPV16 transgenic mice. Am. J. Pathol. *149*, 1899–1917.

Elson, D.A., Riley, R.R., Lacey, A., Thordarson, G., Talamantes, F.J., and Arbeit, J.M. (2000). Sensitivity of the cervical transformation zone to estrogen-induced squamous carcinogenesis. Cancer Res. *60*, 1267–1275.

Elson, D.A., Thurston, G., Huang, L.E., Ginzinger, D.G., McDonald, D.M., Johnson, R.S., and Arbeit, J.M. (2001). Induction of hypervascularity without leakage or inflammation in transgenic mice overexpressing hypoxia-inducible factor-1alpha. Genes Dev. *15*, 2520–2532.

Engel, J.C., Doyle, P.S., Hsieh, I., and McKerrow, J.H. (1998). Cysteine protease inhibitors cure an experimental Trypanosoma cruzi infection. J. Exp. Med. *188*, 725–734.

Foghsgaard, L., Wissing, D., Mauch, D., Lademann, U., Bastholm, L., Boes, M., Elling, F., Leist, M., and Jaattela, M. (2001). Cathepsin B acts as a dominant execution protease in tumor cell apoptosis induced by tumor necrosis factor. J. Cell Biol. *153*, 999–1010.

Folkman, J., Watson, K., Ingber, D., and Hanahan, D. (1989). Induction of angiogenesis during the transition from hyperplasia to neoplasia. Nature *339*, 58–61.

Greenbaum, D., Medzihradszky, K.F., Burlingame, A., and Bogyo, M. (2000). Epoxide electrophiles as activity-dependent cysteine protease profiling and discovery tools. Chem. Biol. *7*, 569–581.

Greenbaum, D., Baruch, A., Hayrapetian, L., Darula, Z., Burlingame, A., Medzihradszky, K.F., and Bogyo, M. (2002). Chemical approaches for functionally probing the proteome. Mol. Cell. Proteomics *1*, 60–68.

Hanahan, D. (1985). Heritable formation of pancreatic beta-cell tumours in transgenic mice expressing recombinant insulin/simian virus 40 oncogenes. Nature *315*, 115–122.

Hanahan, D., and Weinberg, R.A. (2000). The hallmarks of cancer. Cell *100*, 57–70.

Holash, J., Maisonpierre, P.C., Compton, D., Boland, P., Alexander, C.R., Zagzag, D., Yancopoulos, G.D., and Wiegand, S.J. (1999). Vessel cooption, regression, and growth in tumors mediated by angiopoietins and VEGF. Science *284*, 1994–1998.

Huh, C.G., Hakansson, K., Nathanson, C.M., Thorgeirsson, U.P., Jonsson, N., Grubb, A., Abrahamson, M., and Karlsson, S. (1999). Decreased metastatic spread in mice homozygous for a null allele of the cystatin C protease inhibitor gene. Mol. Pathol. *52*, 332–340.

Inoue, M., Hager, J.H., Ferrara, N., Gerber, H.P., and Hanahan, D. (2002). VEGF-A has a critical, nonredundant role in angiogenic switching and pancreatic beta cell carcinogenesis. Cancer Cell *1*, 193–202.

Ito, K., Okamoto, I., Araki, N., Kawano, Y., Nakao, M., Fujiyama, S., Tomita, K., Mimori, T., and Saya, H. (1999). Calcium influx triggers the sequential proteolysis of extracellular and cytoplasmic domains of E-cadherin, leading to loss of beta-catenin from cell-cell contacts. Oncogene *18*, 7080–7090.

Kalluri, R. (2003). Basement membranes: structure, assembly and role in tumour angiogenesis. Nat. Rev. Cancer *3*, 422–433.

Kinzler, K.W., and Vogelstein, B. (1996). Lessons from hereditary colorectal cancer. Cell *87*, 159–170.

Koblinski, J.E., Ahram, M., and Sloane, B.F. (2000). Unraveling the role of proteases in cancer. Clin. Chim. Acta *291*, 113–135.

Koblinski, J.E., Dosescu, J., Sameni, M., Moin, K., Clark, K., and Sloane, B.F. (2002). Interaction of human breast fibroblasts with collagen I increases secretion of procathepsin B. J. Biol. Chem. *277*, 32220–32227.

Konduri, S.D., Yanamandra, N., Siddique, K., Joseph, A., Dinh, D.H., Olivero, W.C., Gujrati, M., Kouraklis, G., Swaroop, A., Kyritsis, A.P., and Rao, J.S. (2002). Modulation of cystatin C expression impairs the invasive and tumorigenic potential of human glioblastoma cells. Oncogene *21*, 8705–8712.

Lah, T.T., and Kos, J. (1998). Cysteine proteinases in cancer progression and their clinical relevance for prognosis. Biol. Chem. *379*, 125–130.

Lopez, T., and Hanahan, D. (2002). Elevated levels of IGF-1 receptor convey invasive and metastatic capability in a mouse model of pancreatic islet tumorigenesis. Cancer Cell *1*, 339–353.

McKerrow, J.H., Engel, J.C., and Caffrey, C.R. (1999). Cysteine protease inhibitors as chemotherapy for parasitic infections. Bioorg. Med. Chem. *7*, 639–644.

Meara, J.P., and Rich, D.H. (1996). Mechanistic studies on the inactivation of papain by epoxysuccinyl inhibitors. J. Med. Chem. *39*, 3357–3366.

Morita, M., Yoshiuchi, N., Arakawa, H., and Nishimura, S. (1999). CMAP: a novel cystatin-like gene involved in liver metastasis. Cancer Res. *59*, 151–158.

Mort, J.S., Recklies, A.D., and Poole, A.R. (1985). Release of cathepsin B precursors from human and murine tumours. Prog. Clin. Biol. Res. *180*, 243–245.

Naik, P., Karrim, J., and Hanahan, D. (1996). The rise and fall of apoptosis during multistage tumorigenesis: down-modulation contributes to tumor progression from angiogenic progenitors. Genes Dev. *10*, 2105–2116.

Parangi, S., Dietrich, W., Christofori, G., Lander, E.S., and Hanahan, D. (1995). Tumor suppressor loci on mouse chromosomes 9 and 16 are lost at distinct stages of tumorigenesis in a transgenic model of islet cell carcinoma. Cancer Res. *55*, 6071–6076.

Perl, A.K., Wilgenbus, P., Dahl, U., Semb, H., and Christofori, G. (1998). A causal role for E-cadherin in the transition from adenoma to carcinoma. Nature *392*, 190–193.

Rao, J.S. (2003). Molecular mechanisms of glioma invasiveness: the role of proteases. Nat. Rev. Cancer *3*, 489–501.

Recklies, A.D., White, C., Mitchell, J., and Poole, A.R. (1985). Secretion of a cysteine proteinase from a hormone-independent cell population of cultured explants of murine mammary gland. Cancer Res. *45*, 2294–2301.

Rios-Doria, J., Day, K.C., Kuefer, R., Rashid, M.G., Chinnaiyan, A.M., Rubin, M.A., and Day, M.L. (2003). The role of calpain in the proteolytic cleavage of E-cadherin in prostate and mammary epithelial cells. J. Biol. Chem. *278*, 1372–1379.

Roshy, S., Sloane, B.F., and Moin, K. (2003). Pericellular cathepsin B and malignant progression. Cancer Metastasis Rev. *22*, 271–286.

Shi, G.P., Munger, J.S., Meara, J.P., Rich, D.H., and Chapman, H.A. (1992). Molecular cloning and expression of human alveolar macrophage cathepsin S, an elastinolytic cysteine protease. J. Biol. Chem. *267*, 7258–7262.

Shi, G.P., Sukhova, G.K., Kuzuya, M., Ye, Q., Du, J., Zhang, Y., Pan, J.H., Lu, M.L., Cheng, X.W., Iguchi, A., et al. (2003). Deficiency of the cysteine protease cathepsin S impairs microvessel growth. Circ. Res. *92*, 493–500.

Shridhar, R., Zhang, J., Song, J., Booth, B.A., Kevil, C.G., Sotiropoulou, G., Sloane, B.F., and Keppler, D. (2003). Cystatin M suppresses the malignant phenotype of human MDA-MB-435S cells. Oncogene, in press.

Smith-McCune, K., Zhu, Y.H., Hanahan, D., and Arbeit, J. (1997). Cross-species comparison of angiogenesis during the premalignant stages of squamous carcinogenesis in the human cervix and K14–HPV16 transgenic mice. Cancer Res. *57*, 1294–1300.

Strathdee, G. (2002). Epigenetic versus genetic alterations in the inactivation of E-cadherin. Semin. Cancer Biol. *12*, 373–379.

Tamayo, P., Slonim, D., Mesirov, J., Zhu, Q., Kitareewan, S., Dmitrovsky, E., Lander, E.S., and Golub, T.R. (1999). Interpreting patterns of gene expression with self-organizing maps: methods and application to hematopoietic differentiation. Proc. Natl. Acad. Sci. USA *96*, 2907–2912.

Tung, C.H., Mahmood, U., Bredow, S., and Weissleder, R. (2000). In vivo imaging of proteolytic enzyme activity using a novel molecular reporter. Cancer Res. *60*, 4953–4958.

Turk, V., Turk, B., and Turk, D. (2001). Lysosomal cysteine proteases: facts and opportunities. EMBO J. *20*, 4629–4633.

Turk, V., Turk, B., Guncar, G., Turk, D., and Kos, J. (2002). Lysosomal cathepsins: structure, role in antigen processing and presentation, and cancer. Adv. Enzyme Regul. *42*, 285–303.

Utsunomiya, T., Hara, Y., Kataoka, A., Morita, M., Arakawa, H., Mori, M., and Nishimura, S. (2002). Cystatin-like metastasis-associated protein mRNA expression in human colorectal cancer is associated with both liver metastasis and patient survival. Clin. Cancer Res. *8*, 2591–2594.

Vleminckx, K., Vakaet, L., Jr., Mareel, M., Fiers, W., and van Roy, F. (1991). Genetic manipulation of E-cadherin expression by epithelial tumor cells reveals an invasion suppressor role. Cell *66*, 107–119.

Wu, X., and Pandolfi, P.P. (2001). Mouse models for multistep tumorigenesis. Trends Cell Biol. *11*, S2–S9.

Yan, S., Sameni, M., and Sloane, B.F. (1998). Cathepsin B and human tumor progression. Biol. Chem. *379*, 113–123.

Yasothornsrikul, S., Greenbaum, D., Medzihradszky, K.F., Toneff, T., Bundey, R., Miller, R., Schilling, B., Petermann, I., Dehnert, J., Logvinova, A., et al. (2003). Cathepsin L in secretory vesicles functions as a prohormone-processing enzyme for production of the enkephalin peptide neurotransmitter. Proc. Natl. Acad. Sci. USA *100*, 9590–9595.